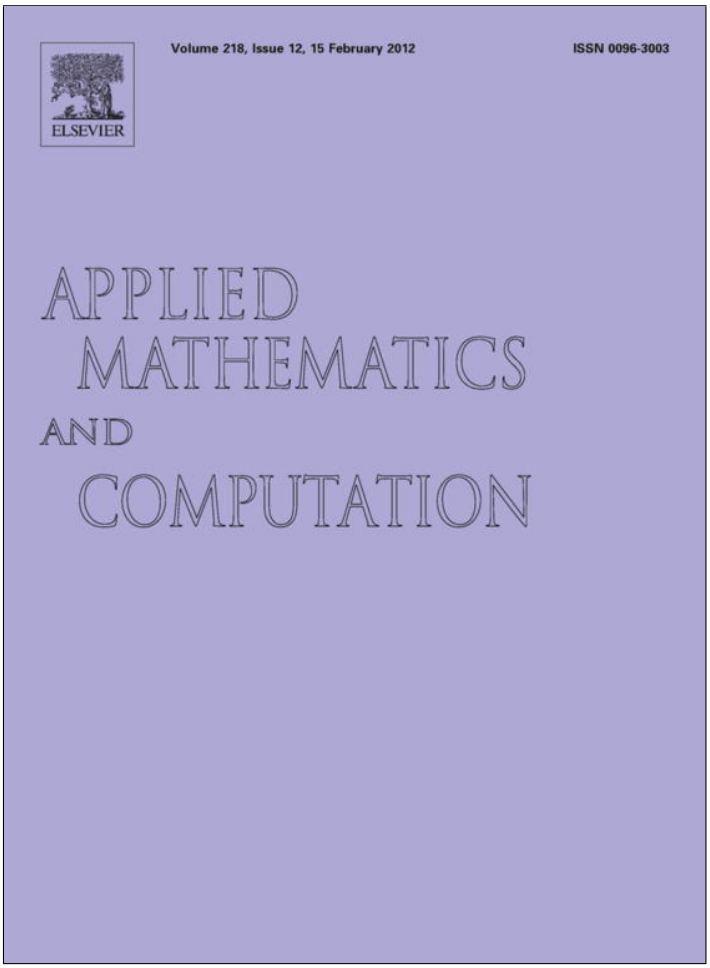

Applied Mathematics and Computation 218 (2012) 6666–6676

Contents lists available at SciVerse ScienceDirect

Applied Mathematics and Computation

journal homepage: www.elsevier.com/locate/amc

High-order non-reflecting boundary conditions for dispersive waves in polar coordinates using spectral elements

Joseph M. Lindquist, Beny Neta *, Francis X. Giraldo

Department of Applied Mathematics, Naval Postgraduate School, 833 Dyer Road, Monterey, CA 93943, United States

ARTICLE INFO

Keywords:
Klein–Gordon equation
Polar coordinates
Advection
Dispersion
High-order
Non-reflecting boundary condition
Spectral elements

ABSTRACT

High-order non-reflecting boundary conditions are introduced to create a finite computational space and for the solution of dispersive waves using a spectral element formulation with high-order time integration. Numerical examples are used to demonstrate the synergy of using high-order spatial, time, and boundary discretization. We show that by balancing all numerical errors involved, high-order accuracy can be achieved for unbounded domain problems in polar coordinate systems.

Published by Elsevier Inc.

1. Introduction

The numerical solution of a wave propagation problem in a very large or unbounded domain provides a challenging computational difficulty – namely, solving the problem on a finite computational domain while maintaining the true *essence* of the solution. One of the modern techniques that has garnered a significant amount of attention in handling this challenge is the absorbing or non-reflecting boundary condition (NRBC) method. In using this method, the original infinite domain is truncated by an artificial boundary $\mathcal{B}$, resulting in a finite computational domain Ω and the residual domain D.

When truncating the domain, the modeler must devise boundary conditions for the truncated domain. Of course, by imposing a boundary where one does not physically exist, the problem is changed – and unless chosen carefully, would certainly be expected to pollute the solution as the problem evolves and impinges on the boundary. For this reason, much effort has and continues to be exerted on finding stable, efficient, accurate and practical means of reducing this reflection through so-called NRBCs [1].

Several *high-order* NRBCs have been devised to reduce spurious reflections that would pollute the solution. Beginning in the late 1980's, the well-known Engquist–Majda [2] and Bayliss–Turkel conditions [3] gave way to Collino's [4] low derivative, auxiliary variable formulation for the 2D scalar wave equation. This sparked a flurry of activity in an effort to find quality, high-order NRBCs that were easily implementable. See [5,6] for reviews on the subject. See also Higdon's papers [7,8], Givoli–Neta [9,10] and Neta et al. [11].

The Givoli–Neta (G–N) auxiliary formulation of the Higdon NRBC was implemented on a reduced form of the linearized shallow water equations (SWE) under non-zero advection. This formulation has been previously demonstrated in a finite difference formulation to *arbitrarily high* NRBC order [12], however, accuracy gains realized by increasing the NRBC ceased after order 2. The formulation used by Lindquist et al. [13] remedied this limitation by using a high-order treatment of space (SE) and time (Runge–Kutta) to show the benefits of using the high-order boundary (G–N) scheme. Spectral elements methods used recently by Mitra and Gopalakrishnan [14] and Vinod et al. [15] to solve wave propagation problem and by Dorao and

* Corresponding author.
E-mail addresses: joseph.lindquist@us.army.mil (J.M. Lindquist), bneta@nps.edu (B. Neta), fxgirald@nps.edu (F.X. Giraldo).

0096-3003/$ - see front matter Published by Elsevier Inc.
doi:10.1016/j.amc.2011.12.023

Jakobsen [16] for incompressible flow. Tohumoglu [17] has applied spectral analysis for periodically time varying discrete time systems.

In this paper, the interior and boundary formulations are discretized using high-order basis functions in a stable, equal-order interpolation scheme for all the variables (this does not violate the inf–sup condition). High-order time integration is performed as well in an effort to balance all of the errors involved with the numerical solution. The computational effort associated with the high-order boundary scheme can be shown to grow only *linearly* with the order [18].

It should be noted that the only other spectral element, high-order boundary approach are Kucherov and Givoli [19] and Lindquist et al. [20,13]. Kucherov and Givoli demonstrate exponential error convergence of the classical wave equation on a semi-infinite channel when solved using spectral elements and high order boundary treatment (using the H–W boundary scheme). They further show how the spectral element formulation allows the NRBC to realize its true potential, prior masked by low order numerical schemes. They note that, "Although it is generally felt that there is no need to treat the time domain 'spectrally' like the spatial domain, [they] feel that a consistently high-order treatment requires that the *entire* approximation be spectral, i.e. the convergence of all three types of error – the spatial and temporal discretization errors and the ABC error – be exponential." [19].

Subsequent spectral element and boundary work by the current authors [20] using the G–N formulation of the dispersive wave equation on a semi-infinite channel showed similar results to those presented by Kucherov and Givoli and how a high-order treatment of the time domain (up to order 10) produces additional improvements. These improvements, however, have their limits thus confirming the hypothesis of Kucherov and Givoli. The key difference in that work is that we extend the high order space, boundary *and* time integration results previously demonstrated in a non-zero advection setting to one where the wave medium is not at rest.

The early work with auxiliary variables in Cartesian coordinates encounters a difficulty at the corners. This was alleviated in the case of the wave equation. This remedy was not possible when one includes dispersion. In order to avoid corners, Lindquist [21] has considered several possibilities and arrived at the conclusion that the best possibility is to use cylindrical or spherical coordinate systems. In the case of cylindrical or spherical coordinate systems, one cannot use the auxiliary functions suggested for the Cartesian coordinate system. The reason is that only in the latter the coefficients are constant. To overcome this, van Joolen et al. [22] extended the Hagstrom–Hariharan (HH) conditions to dispersive media. Here we show how to implement this idea. The following is the outline of the rest of this paper. In Section 2, the problem under investigation is stated. In Section 3, an overview of the auxiliary formulation is presented. In Section 4, a SE semi-discrete formulation that incorporates the NRBC with any desired order is constructed. In Section 5 the time-integrator used to March the equations in time is discussed. The performance of the method is demonstrated in Section 6 via numerical examples.

2. Statement of the problem

To motivate the problem under consideration, consider the SWE (see e.g. [23]):

$$\begin{aligned} &\partial_t u + u\partial_x u + v\partial_y u - f v = -g\partial_x h,\\ &\partial_t v + u\partial_x v + v\partial_y v + fu = -g\partial_y h,\\ &\partial_t h + \partial_x(Hu) + \partial_y(Hv) = 0. \end{aligned} \tag{1}$$

We use the following shorthand for partial derivatives

$$\partial_a^i = \frac{\partial^i}{\partial a^i}.$$

The shallow water model in its current form is non-linear. We have three state variables: $u(x,y,t)$ and $v(x,y,t)$ are the unknown velocities in the x and y directions and $h(x,y,t)$ is the water depth above a reference value. Further, H is the water depth as shown in Fig. 1 such that $H = h_B + h$, f is the Coriolis parameter, and g is the gravity acceleration.

Now, suppose that the bottom topography is flat such that h_B is constant and u and v can be described by a constant *mean* term and a small $O(\delta)$ deviation from that value, i.e.

$$u = U + u^* \quad v = V + v^*.$$

To be clear, U and V are the mean velocities with respect to the coordinate axes. Using these substitutions and neglecting any $O(\delta^2)$ terms results in the linearized form of the SWE:

$$\begin{aligned} &\partial_t u^* + U\partial_x u^* + V\partial_y u^* - f(V + v^*) = -g\partial_x h,\\ &\partial_t v^* + U\partial_x v^* + V\partial_y v^* + f(U + u^*) = -g\partial_y h,\\ &\partial_t h + U\partial_x h + V\partial_y h + h_B(\partial_x u^* + \partial_y v^*) = 0. \end{aligned} \tag{2}$$

van Joolen shows in [24], how, using the operator:

$$\frac{D}{Dt} = \frac{\partial}{\partial t} + U\frac{\partial}{\partial x} + V\frac{\partial}{\partial y},$$

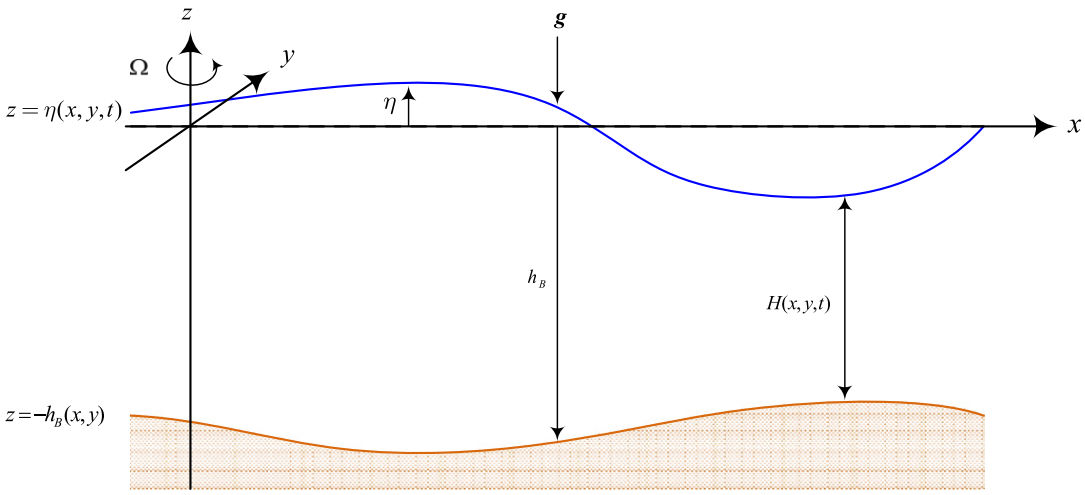

Fig. 1. The shallow water model with irregular bottom topography. Adapted from [23, p. 58].

the SWE can be reduced to a single variable Klein Gordon equation (KGE) equivalent for the wave perturbation h under non-zero, constant advection velocities U and V. Once h has been found, the unknown velocities can be computed in a similar manner (see [23] for details). The current paper seeks to numerically solve this two-dimensional advective, dispersive wave equation:

$$\partial_t^2 h + \left(U^2 - C_0^2\right)\partial_x^2 h + \left(V^2 - C_0^2\right)\partial_y^2 h + 2U\partial_{xt}^2 h + 2V\partial_{yt}^2 h + 2UV\partial_{xy}^2 h + f^2 h = 0, \tag{3}$$

where $C_0^2 = gH$, using continuous Galerkin methods.

While the assumptions for this reduced form of the SWE may undermine the predictive capability of the already simplified equations of fluid motion, the advective KGE serves as an important test-bed to extend and improve non-reflecting boundary conditions for wave propagation in a non-static environment. When shown to improve performance in test cases as those presented here, these conditions will then be extended to the full linearized SWE system and further to include non-linear effects.

3. Hagstrom and Hariharan auxiliary variable formulation

The boundary condition devised by Hagstrom and Hariharan [25] provides a systematic approach for constructing boundary conditions for the standard two-dimensional wave equation. The condition is based on the asymptotic series representation (which does not converge at any fixed radius) for an outgoing solution of the wave equation (in polar coordinates)

$$\frac{1}{c_0^2}\frac{\partial^2 h}{\partial t^2} = \frac{\partial^2 h}{\partial r^2} + \frac{1}{r}\frac{\partial h}{\partial r} + \frac{1}{r^2}\frac{\partial^2 h}{\partial \theta^2}. \tag{4}$$

Since the boundary condition is asymptotic by nature, valid for large radial distances – this implies that larger radial distances should provide better NRBC convergence. Thompson et al. make the observation that "... for practical problems, truncating the asymptotic expansion after [J] terms provides solutions with errors well below that of the discretization error" [26]. Here, we seek to significantly reduce the discretization error by employing spectral elements to find the true error convergence properties of the NRBC. In developing the boundary condition, Hagstrom and Hariharan construct a sequence of operators that approximately annihilate the residual of the preceding element in the sequence, viewed as a function on the artificial boundary. The sequence begins with a first-order Bayliss–Turkel operator discussed in [3]. The boundary condition takes the form:

$$\frac{\partial h}{\partial r} = \phi_1 - \frac{1}{c_0}\frac{\partial h}{\partial t} - \frac{1}{2r}h, \tag{5}$$

$$\phi_{j+1} = \frac{1}{c_0}\frac{\partial \phi_j}{\partial t} + \frac{j}{r}\phi_j - \frac{\left(j-\frac{1}{2}\right)^2}{4r^2}\phi_{j-1} - \frac{1}{4r^2}\frac{\partial^2 \phi_{j-1}}{\partial \theta^2}, \quad j = 1, \ldots, J-1, \tag{6}$$

where

$$\phi_0 \equiv 2h \quad \text{and} \quad \phi_J \equiv 0.$$

At first glance, this boundary formulation suggests that we should develop a "new" spectral element formulation for the wave equation cast in polar coordinates. If we did this, however, we would then require a polar grid that would introduce additional complications such as the method of dealing with the degenerate quadrilaterals that inevitably occur at the center

of the grid. Of course there are ways to overcome these obstacles, but it would be much more convenient to cast the problem in the same framework already developed. In other words, we seek to implement this boundary condition (presented in polar form) in our unstructured quadrilateral formulation of the wave equation (in Cartesian form).

4. Spectral element method

The spectral element (SE) method is a generalized high-order finite element method where the integration and interpolation points are selected carefully in order to yield accurate but efficient solutions. For this problem, we will discuss two formulations – one for the interior and one for implementing the boundary conditions.

4.1. Interior formulation

First, consider the two-dimensional wave equation (same formulation as presented in (3) with $U = V = 0$)

$$\frac{\partial^2 h}{\partial t^2} - c_0^2 \nabla^2 h + f^2 h = 0. \tag{7}$$

Multiplying by the test functions Ψ_i and integrating over the circular domain yields the weak integral form

$$\int_\Omega \Psi_i \frac{\partial^2 h}{\partial t^2} d\Omega - c_0^2 \int_\Omega \Psi_i \nabla^2 h d\Omega + \int_\Omega \Psi_i f^2 h d\Omega = 0.$$

Transferring the second order spatial derivatives from h to the basis functions via integration by parts and applying the divergence theorem to recast one surface integral term as a boundary integral gives us

$$\int_\Omega \Psi_i \frac{\partial^2 h}{\partial t^2} d\Omega - c_0^2 \int_\Gamma \Psi_i \vec{n} \cdot \nabla h d\Gamma + c_0^2 \int_\Omega \nabla \Psi_i \cdot \nabla h d\Omega + \int_\Omega \Psi_i f^2 h d\Omega = 0. \tag{8}$$

Of note now is that the boundary condition (5) contains a radial derivatives of h that on the circle is precisely the normal derivative $\vec{n} \cdot \nabla h$. This allows direct implementation of the boundary condition into (8) as follows:

$$\int_\Omega \Psi_i \frac{\partial^2 h}{\partial t^2} d\Omega - c_0^2 \int_\Gamma \Psi_i \left(\phi_1 - \frac{1}{c_0} \frac{\partial h}{\partial t} - \frac{1}{2r} h \right) d\Gamma + c_0^2 \int_\Omega \nabla \Psi_i \cdot \nabla h d\Omega + \int_\Omega \Psi_i f^2 h d\Omega = 0. \tag{9}$$

Here, since on the boundary the radius is fixed, the $\frac{1}{2r}$ term may be treated as a constant.

A similar weak form is constructed for the boundary formulation by multiplying (6) by the test functions ζ_i and integrating over Γ yielding (after by integration by parts):

$$\begin{aligned} &\frac{1}{c_0} \int_\Gamma \zeta_i \frac{\partial \phi_j}{\partial t} d\Gamma + \frac{j}{r} \int_\Gamma \zeta_i \phi_j d\Gamma - \frac{\left(j - \frac{1}{2}\right)^2}{4r^2} \int_\Gamma \zeta_i \phi_{j-1} d\Gamma - \frac{1}{4r^2} \zeta_i \frac{\partial \phi_{j-1}}{\partial \theta} \Big|_{start}^{end} + \frac{1}{4r^2} \int_\Gamma \frac{\partial \zeta_i}{\partial \theta} \frac{\partial \phi_{j-1}}{\partial \theta} d\Gamma \\ &= \int_\Gamma \zeta_i \phi_{j+1} d\Gamma, \quad j = 1, 2, \ldots, J-1, \end{aligned} \tag{10}$$

where $\phi_0 = h$. We now use the fact that the boundary is continuous and closed to surmise that the endpoint evaluation term vanishes. The formal problem statement is then: Find $h \in \mathcal{V}$ and $\phi_j \in \mathcal{V}_\Gamma$ where $j = 1, \ldots, J-1$, such that Eqs. (9) and (10) are satisfied $\forall \Psi_i \in \mathcal{V}$ and $\zeta_i \in \mathcal{V}_\Gamma$. Here, the finite-dimensional spectral element spaces (the discrete representations of $\mathcal{V}$ and $\mathcal{V}_\Gamma$) are defined as follows

$$\mathcal{V}_N = \{ \Psi \in H^1(\Omega) : \Psi \in \mathcal{P}_N(\mathrm{I}),\ e = 1, \ldots, N_e \},$$

where

$$\mathcal{P}_N(\mathrm{I}) = span\{ \xi^n \eta^m | m, n \leqslant N, (\xi, \eta) \in \mathrm{I} \}, \quad N \geqslant 1$$

and I is the unit square.

4.2. Galerkin expansion

We now turn our attention to the spatial discretization. First, we expand the solution variables h and ϕ_j using the basis functions as follows:

$$h_N = \sum_{k=1}^{N_p} \Psi_k h^k, \quad \phi_{jN} = \sum_{k=1}^{N_b} \zeta_k \phi_j^k, \quad j = 1, 2, \ldots, J-1. \tag{11}$$

Here, N_p refers to the number of points that Ω is discretized into and N_b refers to the number of points that Γ is discretized into. Next, we substitute these basis function expansions directly into the weak forms, resulting in the following matrix form of the problem:

$$M\ddot{h} = \mathbb{A}\dot{h} + \mathbb{B}h + \mathbb{C}\phi_1, \tag{12}$$

where

$$\begin{aligned} \mathbb{A} &= c_0 B, \\ \mathbb{B} &= -\left(c_0^2 L + \frac{c_0^2}{2r} B + f^2 M\right), \\ \mathbb{C} &= c_0^2 B, \end{aligned} \tag{13}$$

$$M_{ik} = \int_\Omega \Psi_i \Psi_k d\Omega \quad B_{ik} = \int_\Gamma \Psi_i \Psi_k d\Gamma,$$
$$L_{ik} = \int_\Omega \nabla\Psi_i \nabla\Psi_k d\Omega \quad A_{ik} = \int_\Gamma \Psi_i \zeta_k d\Gamma.$$

If we examine the boundary auxiliary variable formulation (10) we see that the selection of appropriate C_j values for the auxiliary variables has not yet been addressed.

It should be noted that van Joolen et al. [27] show that *any* choice of C_j is guaranteed to reduce spurious reflection as the order of the NRBC (J) increases. While we omit the details here, the core of this argument is the computation of a so-called reflection coefficient that is a product of J factors, each of which are less than one. The reflection caused by the artificial boundary *must* decrease as the order of the NRBC increases. They note, "Of course, a good choice for the C_j would lead to better accuracy with a lower order J, but even if the 'wrong' C_j's are taken ... one is still guaranteed to reduce the spurious reflection as the order J increases. [27, p. 1045].

If we now collect the terms on the left and right, we get the matrix form of the problem:

$$\mathbb{E}\dot{\Phi} = \mathbb{F}\Phi + \bar{h}, \tag{14}$$

where

$$M_{ik}^b = \int_\Gamma \zeta_i \zeta_k d\Gamma \quad l_{ik}^b = \int_\Gamma \zeta_i' \zeta_k' d\Gamma,$$

$$\mathbb{E} = \begin{pmatrix} \frac{1}{c_0}M^b & 0 & \dots & 0 \\ 0 & \frac{1}{c_0}M^b & \dots & 0 \\ \vdots & \vdots & \ddots & \vdots \\ 0 & 0 & 0 & \frac{1}{c_0}M^b \end{pmatrix},$$

$$\mathbb{F} = \begin{pmatrix} \frac{1}{r}M^b & -M^b & 0 & \dots & 0 \\ \frac{1}{4r^2}\left(\frac{1}{4}M^b - l\right) & \frac{2}{r}M^b & -M^b & \dots & 0 \\ \vdots & \ddots & \ddots & \ddots & \vdots \\ 0 & 0 & \frac{1}{4r^2}\left(\left(J-\frac{3}{2}\right)^2 M^b - l\right) & \frac{J-2}{r}M^b & -M^b \\ 0 & 0 & 0 & \frac{1}{4r^2}\left(\left(J-\frac{1}{2}\right)^2 M^b - l\right) & \frac{J-1}{r}M^b \end{pmatrix},$$

$$\Phi = \begin{pmatrix} \phi_1 \\ \phi_2 \\ \vdots \\ \phi_{J-1} \end{pmatrix}, \quad \dot{\Phi} = \begin{pmatrix} \dot{\phi}_1 \\ \dot{\phi}_2 \\ \vdots \\ \dot{\phi}_{J-1} \end{pmatrix} \quad \text{and} \quad \bar{h} = \begin{pmatrix} \frac{1}{4r^2}\left(\frac{1}{4}M^b - l\right) \\ 0 \\ \vdots \\ 0 \end{pmatrix}.$$

4.3. Time integration

The formulation outlined in (12) and (14) constitute a system of coupled ODEs that must be solved to yield a solution for $h(x,y,t)$. Since the goal of this analysis is to uncover the "true" gains made by high-order boundary treatment, it is possible that any high-order treatment of the boundary and spatial discretization *without* considering a high-order treatment of the temporal component could mask gains made by a high-order boundary treatment. For this purpose, our approach uses standard kth order Runge–Kutta (RK) methods (up to order 10) to integrate the system in time.

The set-up of this scheme is a standard one, namely, the second order system is expanded to a larger system of first order ODEs, then solved appropriately using the associated RK tableau. For most cases in this analysis (unless otherwise stated)

time integration is performed using a 4th order RK scheme using a time-step chosen to ensure a Courant number of 0.25, where the Courant number is defined:

$$\text{Courant number} = \frac{C_0 \Delta t}{\sqrt{(\Delta x)^2 + (\Delta y)^2}}.$$

Here, Δx and Δy are chosen as the minimum distance between any two points in the x- or y-directions respectively. Additionally, This choice is made since the interpolation points are not uniformly distributed when using spectral elements.

4.4. Results for the HH formulation

A series of experiments was conducted to determine the effect of the HH boundary condition for various SE and NRBC orders. Since the formulation is designed for circular boundaries, we consider only circular boundaries with unstructured grids. In each case, we choose the number of elements to yield approximately 3000 global points. We take a smooth, two-dimensional "oval-shaped" initial condition with shape parameters $\sigma_x = \frac{1}{2}$, $\sigma_y = \frac{1}{3}$, further rotated by an angle of $\theta = \frac{\pi}{6}$. The initial condition used here is:

$$h(x, y, 0) = e^{-(ax^2 + 2bxy + cy^2)}, \quad \dot{h}(x, y, 0) = 0. \tag{15}$$

Here, the parameters a, b, and c are defined as follows:

$$a = \frac{\cos^2\theta}{2\sigma_x^2} + \frac{\sin^2\theta}{2\sigma_y^2} \quad b = -\frac{\sin 2\theta}{4\sigma_x^2} + \frac{\sin 2\theta}{4\sigma_y^2} \quad c = \frac{\sin^2\theta}{2\sigma_x^2} + \frac{\cos^2\theta}{2\sigma_y^2}. \tag{16}$$

Again, the solution is compared to one computed on a larger domain allowing the wave to propagate out of the NRBC domain but not yet impinge on the non-physical boundary used to compute the solution on the larger domain. Qualitative results are shown in Fig. 2 and quantitative L^2_Ω errors are shown for various NRBC orders for SE orders up to 6 in Table 2. No further improvement was observed for SE orders above order 6.

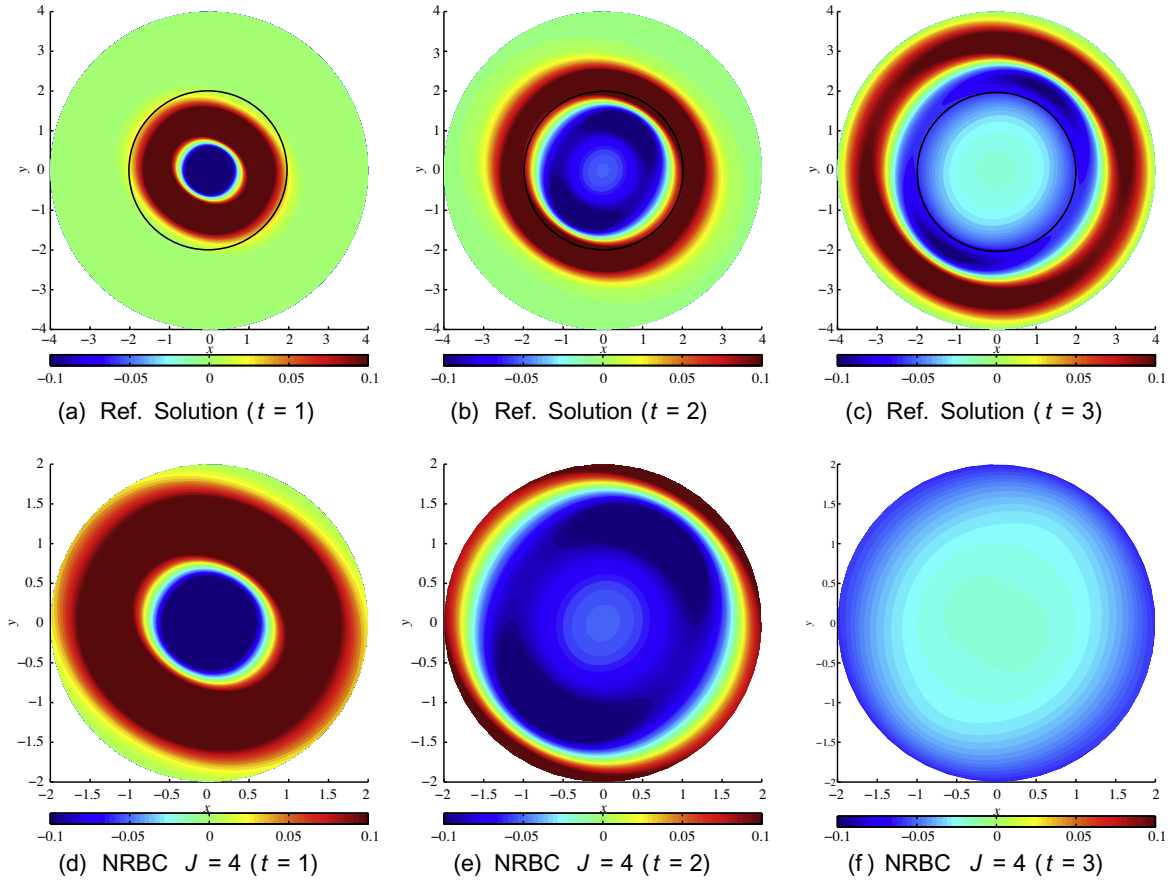

Fig. 2. Open domain, 4th order spectral elements ($J = 4$) using oblique Gaussian initial condition shown for $t = 1, 2, 3$. **Top plots:** contour plots of reference solution solved on extended domain. Superimposed black circle indicates NRBC domain. **Bottom plots:** contour plots of various NRBC boundary configurations using $J = 4$.

4.5. Adjustments to HH to include mild dispersion

The unstructured grid (see e.g. Fig. 3) representation of the HH formulation has been demonstrated to significantly reduce reflection caused by the boundary for the standard wave equation. The question now arises, can this formulation be extended to include dispersive effects such as Coriolis? In [22], van Joolen et al. presented a method to extend the HH formulation for the standard wave equation under mild dispersion. While this formulation was well grounded mathematically it was never implemented. A brief synopsis of their derivation follows with results presented for *mild* dispersion where $f^2 = 0.1$.

We first consider the KGE without advection (in polar coordinates as in the HH derivation):

$$\frac{1}{c_0^2}\frac{\partial^2 h}{\partial t^2} = \frac{\partial^2 h}{\partial r^2} + \frac{1}{r}\frac{\partial h}{\partial r} + \frac{1}{r^2}\frac{\partial^2 h}{\partial \theta^2} - \frac{f^2}{c_0^2}h. \tag{17}$$

As has been previously discussed, in the geophysical context, the dispersion parameter is typically small. We assume here that

$$\frac{f}{c_0 K} \ll 1, \tag{18}$$

where K is a typical wave number appearing in the solution. Now, apply the Fourier transform to (4) and (17) in time to yield:

$$\frac{\omega^2}{c_0^2}\hat{h} + \frac{\partial^2 \hat{h}}{\partial r^2} + \frac{1}{r}\frac{\partial \hat{h}}{\partial r} + \frac{1}{r^2}\frac{\partial^2 \hat{h}}{\partial \theta^2} = 0 \quad \text{Wave},$$

$$\left(\frac{\omega^2}{c_0^2} - \frac{f^2}{c_0^2}\right)\hat{h} + \frac{\partial^2 \hat{h}}{\partial r^2} + \frac{1}{r}\frac{\partial \hat{h}}{\partial r} + \frac{1}{r^2}\frac{\partial^2 \hat{h}}{\partial \theta^2} = 0 \quad \text{Klein–Gordon},$$

where ω is the frequency and $\hat{h}$ is the frequency domain representation of h. In both cases, we obtain the Helmholtz equation:

$$\overline{K}^2\hat{h} + \frac{\partial^2 \hat{h}}{\partial r^2} + \frac{1}{r}\frac{\partial \hat{h}}{\partial r} + \frac{1}{r^2}\frac{\partial^2 \hat{h}}{\partial \theta^2} = 0.$$

In the non-dispersive case, $\overline{K} = \frac{\omega}{c_0} \equiv K$ and $\overline{K} = \sqrt{K^2 - \frac{f^2}{c_0^2}}$ in the dispersive case. In order to facilitate the conversion back to the time domain, we now consider a Taylor series approximation to the square root term found in the dispersive case, i.e.,

$$\sqrt{1-x} = 1 - \frac{1}{2}x + O(x^2).$$

Provided that x is small, we can truncate the $O(x^2)$ terms. In our case, from (18) we can reasonably make this assumption yielding for the dispersive case:

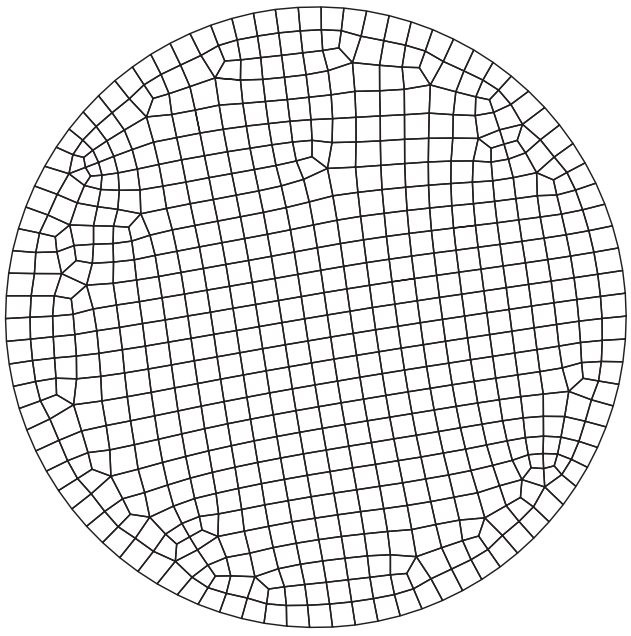

Fig. 3. Unstructured grid.

$$\frac{\overline{K}}{K} = \sqrt{1 - \frac{f^2}{c_0^2 K^2}} \approx 1 - \frac{f^2}{2c_0^2 K^2} \Rightarrow \overline{K} \approx K - \frac{f^2}{2c_0^2 K}.$$

We now see that in the frequency domain, an equation valid in the non-dispersive case is valid in the dispersive case if we make the replacement:

$$K \to \sqrt{K^2 - \frac{f^2}{c_0^2}} \approx K - \frac{f^2}{2c_0^2 K}. \tag{19}$$

We now turn our attention to the boundary condition (5) and (6) that we Fourier transform in time to yield:

$$-iK\hat{h} + \frac{\partial \hat{h}}{\partial r} + \frac{1}{2r}\hat{h} = \hat{\phi}_1, \tag{20}$$

$$-iK\hat{\phi}_j + \frac{j}{r}\hat{\phi}_j - \frac{\left(j-\frac{1}{2}\right)^2}{4r^2}\hat{\phi}_{j-1} - \frac{1}{4r^2}\frac{\partial^2 \hat{\phi}_{j-1}}{\partial \theta^2} = \hat{\phi}_{j+1}, \quad j = 1, \ldots, J-1. \tag{21}$$

Making the substitution (19), we obtain the dispersive version of the HH formulation in the frequency domain, i.e.,

$$-iK\hat{h} + \frac{if^2}{2c_0^2 K}\hat{h} + \frac{\partial \hat{h}}{\partial r} + \frac{1}{2r}\hat{h} = \hat{\phi}_1,$$

$$-iK\hat{\phi}_j + \frac{if^2}{2c_0^2 K}\hat{\phi}_j + \frac{j}{r}\hat{\phi}_j - \frac{\left(j-\frac{1}{2}\right)^2}{4r^2}\hat{\phi}_{j-1} - \frac{1}{4r^2}\frac{\partial^2 \hat{\phi}_{j-1}}{\partial \theta^2} = \hat{\phi}_{j+1}, \quad j = 1, \ldots, J-1.$$

Transforming these equations back into the time domain results in the final HH boundary formulation for the KGE:

$$\frac{1}{c_0}\frac{\partial h}{\partial t} + \frac{f^2}{2c_0}\underbrace{\int_0^t h(\tau)d\tau}_{m(t)} + \frac{\partial h}{\partial r} + \frac{1}{2r}h = \phi_1, \tag{22}$$

$$\frac{1}{c_0}\frac{\partial \phi_j}{\partial t} + \frac{f^2}{2c_0}\underbrace{\int_0^t \phi_j(\tau)d\tau}_{n(t)} + \frac{j}{r}\phi_j - \frac{\left(j-\frac{1}{2}\right)^2}{4r^2}\phi_{j-1} - \frac{1}{4r^2}\frac{\partial^2 \phi_{j-1}}{\partial \theta^2} = \phi_{j+1}, \tag{23}$$

where

$$j = 1, \ldots, J-1, \quad \phi_0 \equiv 2h \quad \text{and} \quad \phi_J \equiv 0.$$

It should be noted that van Joolen et al. [22] show how $m(t)$ and $n(t)$ can be calculated in each time-step to keep the boundary condition local in time without having to store and operate on the history of the solution. For this analysis, a simple trapezoidal approximation was used to approximate the integral.

The weak form of the formulation is now constructed. We consider the KGE in its general form:

$$\frac{\partial^2 h}{\partial t^2} - c_0^2 \nabla^2 h + f^2 h = 0.$$

Multiplying by the test functions Ψ_i and integrating over the circular domain yields the weak integral form

$$\int_\Omega \Psi_i \frac{\partial^2 h}{\partial t^2} d\Omega - c_0^2 \int_\Omega \Psi_i \nabla^2 h d\Omega + f^2 \int_\Omega \Psi_i h d\Omega = 0.$$

Transferring the second order spatial derivatives from h to the basis functions via integration by parts and applying the divergence theorem to recast one surface integral term as a boundary integral gives us

$$\int_\Omega \Psi_i \frac{\partial^2 h}{\partial t^2} d\Omega - c_0^2 \int_\Gamma \Psi_i \vec{n} \cdot \nabla h d\Omega + c_0^2 \int_\Omega \nabla \Psi_i \cdot \nabla h d\Omega + f^2 \int_\Omega \Psi_i h d\Omega = 0. \tag{24}$$

Of note now is that the boundary condition (22) contains a radial derivatives of h that on the circle is precisely the normal derivative $\vec{n} \cdot \nabla h$. This allows direct implementation of the boundary condition into (24) as follows:

$$\int_\Omega \Psi_i \frac{\partial^2 h}{\partial t^2} d\Omega - c_0^2 \int_\Gamma \Psi_i \left(\phi_1 - \frac{1}{c_0}\frac{\partial h}{\partial t} - \frac{1}{2r}h - \frac{f^2}{2c_0}m(t)\right) d\Omega + c_0^2 \int_\Omega \nabla \Psi_i \cdot \nabla h d\Omega + f^2 \int_\Omega \Psi_i h d\Omega = 0. \tag{25}$$

Here, since on the boundary the radius is fixed, the $\frac{1}{2r}$ term may be treated as a constant.

A similar weak form is constructed for the boundary formulation by multiplying (23) by the test functions ζ_i and integrating over Γ yielding (after integration by parts):

$$\frac{1}{c_0}\int_\Gamma \zeta_i \frac{\partial \phi_j}{\partial t} d\Gamma + \frac{f^2}{2c_0}\int_\Gamma \zeta_i n(t) d\Gamma + \frac{j}{r}\int_\Gamma \zeta_i \phi_j d\Gamma - \frac{\left(j-\frac{1}{2}\right)^2}{4r^2}\int_\Gamma \zeta_i \phi_{j-1} d\Gamma - \frac{1}{4r^2}\zeta_i \frac{\partial \phi_{j-1}}{\partial \theta}\Big|_{start}^{end} + \frac{1}{4r^2}\int_\Gamma \frac{\partial \zeta_i}{\partial \theta}\frac{\partial \phi_{j-1}}{\partial \theta} d\Gamma = \int_\Gamma \zeta_i \phi_{j+1} d\Gamma. \quad (26)$$

We now use the fact that the boundary is continuous and closed to surmise that the endpoint evaluation term vanishes. The formal problem statement is then: Find $h \in \mathcal{V}$ and $\phi_j \in \mathcal{V}_\Gamma$ where $j = 1,\ldots,J-1$, such that Eqs. (25) and (26) are satisfied $\forall \Psi_i \in \mathcal{V}$ and $\zeta_i \in \mathcal{V}_\Gamma$.

4.6. Results for HH with dispersion

A series of experiments was conducted to determine the effect of the HH boundary condition extended to include mild dispersion for various SE and NRBC orders. The set-up is identical to the experiments without dispersion, except the dispersion parameter is set to $f^2 = 0.1$. Qualitative results are shown in Fig. 4 and quantitative L^2_Ω errors are shown for various NRBC orders for SE orders up to 6 in Table 1. As in the non-dispersive case, no improvement was observed for SE orders above order 6.

4.7. Effects of time integration technique

At the outset of this work, it was believed that at some point the improvements realized by improving the spatial discretization and NRBC would eventually be limited by the time integration scheme [28]. To this end, the order of the time integration scheme (RK2 -RK10) was varied to examine the effects of time integration on the accuracy of the solution. As has already been presented, gains made by increasing the order of the NRBC halt for lower order (second order) spectral elements after $J = 5$. Even for high order (order 8 and 16) spectral elements, the gains made by increasing the order of the NRBC are limited at some point using RK4. In [20] the authors showed that high-order time integration allowed boundary gains to improve solution quality for the KGE under zero advection.

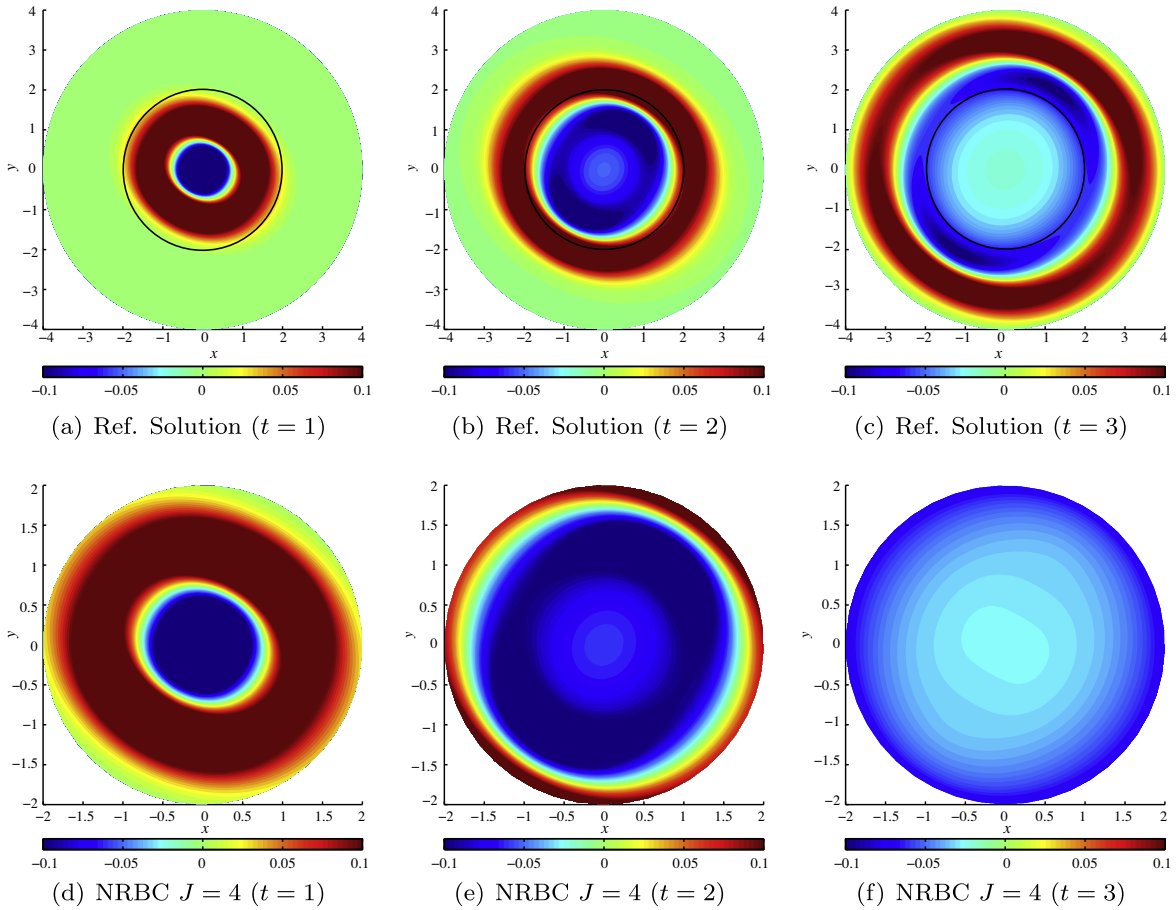

Fig. 4. Open domain, 4th order spectral elements ($J = 4$) using oblique Gaussian initial condition shown for $t = 1,2,3$ under dispersion $f^2 = 0.1$. **Top plots:** contour plots of reference solution solved on extended domain. Superimposed black circle indicates NRBC domain. **Bottom plots:** contour plots of various NRBC boundary configurations using $J = 4$.

Table 1
L^2_Ω error as a function of NRBC order for Hagstrom Hariharan NRBC formulation using various spectral element orders on the circular NRBC domain. Oblique Gaussian initial condition is used with dispersion parameter set to $f^2 = 0.1$.

NRBC order	L^2_Ω error linear elements	L^2_Ω error order 2 elements	L^2_Ω error order 4 elements	L^2_Ω error order 6 elements
$J = 1$	0.07290	0.03555	0.03369	0.03293
$J = 2$	0.02684	0.00371	0.00283	0.00248
$J = 3$	0.01869	0.00258	0.00192	0.00204
$J = 4$	0.01759	0.00243	0.00186	0.00157
$J = 5$	0.01744	0.00240	0.00181	0.00154
$J = 10$	0.01742	0.00240	0.00180	0.00153
$J = 20$	0.01742	0.00240	0.00180	0.00153

Table 2
L^2_Ω error as a function of NRBC order for Hagstrom Hariharan NRBC formulation using various spectral element orders on the circular NRBC domain. Oblique Gaussian initial condition is used.

NRBC order	L^2_Ω error linear elements	L^2_Ω error order 2 elements	L^2_Ω error order 4 elements	L^2_Ω error order 6 elements
$J = 1$	0.09310	0.04772	0.04555	0.04485
$J = 2$	0.03381	0.00465	0.00355	0.00315
$J = 3$	0.02355	0.00324	0.00243	0.00259
$J = 4$	0.02217	0.00305	0.00236	0.00201
$J = 5$	0.02198	0.00302	0.00230	0.00196
$J = 10$	0.02195	0.00302	0.00228	0.00196
$J = 20$	0.02195	0.00302	0.00228	0.00196

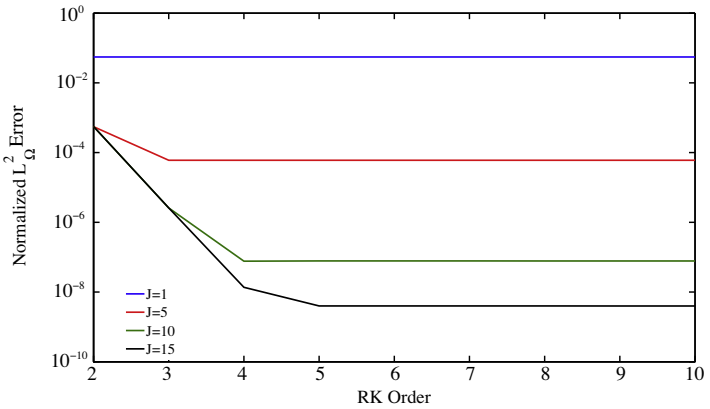

Fig. 5. Semi-infinite channel L^2_Ω error versus RK time integration order using various order NRBCs. Domain is discretized into 9409 points for 8th order spectral elements with advection velocities $U = 0.75$, $V = 0.0$ and dispersion parameter $f^2 = 1$.

For this experiment, consider the KGE on a semi-infinite domain with $h = 0$ on Γ_W. To ensure that any boundary or time effects are not masked by the interior discretization, we consider 8th order spectral elements discretized into 9409 global points. The Gaussian initial condition is used and is evaluated until $t = 3$. The reference solution in this case was computed as described previously, except that time integration was performed with a 10th order Runge–Kutta scheme (RK10) using a time-step chosen to ensure a Courant number of 0.1. Further, to exaggerate the issue of advection and dispersion, we consider the case where $U = 0.75$ and $f^2 = 1$.

As can be observed in Fig. 5, gains made by improving the time integration matter only if combined with high-order treatment of the boundary. Conversely – gains using high-order treatment of the boundary can only be realized if there is a *sufficiently* high-order treatment of the time integration. While this analysis conducted time integration using up to RK10 (18 stages), RK4 or RK5 appears to be sufficient in exploiting gains when using high-order (up to $J = 15$) boundary treatment. It should be noted that these results (error on the order of 10^{-9}) cannot be observed unless high-order treatment of the interior also accompanies the high-order treatment of the boundary **and** time. Several experiments were conducted which varied the order of the interior, boundary and time integration. The clear result was that without high-order treatment of all components in concert, convergence to the reference solution is stalled.

While these results are for a specific problem (KGE with advection), we believe that the principle of a **balanced** approach to all components (interior, boundary and time) is a sound, extensible procedure for any problem. If high-order treatment of

any of the three components is missing, the high-order treatment of the other components is essentially wasted; the results reported here confirm this.

5. Conclusions

In this paper we have considered high order nonreflecting boundary conditions in polar coordinates thus we overcame the corner problem. The numerical examples demonstrated the synergy of using high-order spatial, time, and boundary discretization. It was shown that by balancing all numerical errors involved, high-order accuracy can be achieved for unbounded domain problems in polar coordinate systems.

Acknowledgements

The first author is indebted to the US Army for its support. The authors would like to express their appreciation to the Naval Postgraduate School for its support of this research. Finally, the authors wish to thank the reviewers for their helpful insights, suggestions and comments.

References

[1] D. Givoli, Non-reflecting boundary conditions, Journal of Computational Physics 94 (1) (1991) 1–29, doi:10.1016/0021-9991(91)90135-8.
[2] B. Engquist, A. Majda, Radiation boundary conditions for acoustic and elastic calculations, Communications on Pure and Applied Mathematics 32 (3) (1979) 313–357, doi:10.1002/cpa.3160320303.
[3] A. Bayliss, E. Turkel, Radiation boundary conditions for wave-like equations, Communications on Pure and Applied Mathematics 33 (6) (1980) 707–725, doi:10.1002/cpa.3160330603.
[4] F. Collino, High order absorbing boundary conditions for wave propagation models. Straight line boundary and corner cases, in: R. Kleinman et al. (Eds.), Proceedings of the second International Conference on Mathematical & Numerical Aspects of Wave Propagation, SIAM, Delaware, 1993, pp. 161–171.
[5] S.V. Tsynkov, Numerical solution of problems on unbounded domains. A review, Applied Numerical Mathematics 27 (4) (1998) 465–532, doi:10.1016/S0168-9274(98)00025-7.
[6] T. Hagstrom, Radiation boundary conditions for the numerical simulation of waves, Acta Numerica 8 (-1) (1999) 47–106, doi:10.1017/S0962492900002890.
[7] R.L. Higdon, Absorbing boundary conditions for difference approximations to the multi-dimensional wave equation, Mathematics of Computation 47 (176) (1986) 437–459.
[8] R.L. Higdon, Radiation boundary conditions for dispersive waves, SIAM Journal on Numerical Analysis 31 (1) (1994) 64–100, doi:10.1137/0731004.
[9] D. Givoli, B. Neta, High-order non-reflecting boundary conditions for dispersive waves, Wave Motion 37 (3) (2003) 257–271, doi:10.1016/S0165-2125(02)00074-4.
[10] D. Givoli, B. Neta, High-order non-reflecting boundary scheme for time-dependent waves, Journal of Computational Physics 186 (1) (2003) 24–46, doi:10.1016/S0021-9991(03)00005-6.
[11] B. Neta, V. van Joolen, J.R. Dea, D. Givoli, Application of high-order higdon non-reflecting boundary conditions to linear shallow water models, Communications in Numerical Methods in Engineering 24 (11) (2008) 1459–1466, doi:10.1002/cnm.1044.
[12] V.J. van Joolen, B. Neta, D. Givoli, High-order boundary conditions for linearized shallow water equations with stratification, dispersion and advection, International Journal for Numerical Methods in Fluids 46 (4) (2004) 361–381, doi:10.1002/fld.754.
[13] J.M. Lindquist, F.X. Giraldo, B. Neta, Klein–Gordon equation with advection on unbounded domains using spectral elements and high-order non-reflecting boundary conditions, Applied Mathematics and Computation 217 (2010) 2710–2723.
[14] M. Mitra, S. Gopalakrishnan, Wave propagation analysis in anisotropic plate using wavelet spectral element approach, Journal of Applied Mechanics, Transactions ASME 75 (2008) 145041–145046.
[15] K. Vinod, S. Gopalakrishnan, R. Ganguli, Free vibration and wave propagation analysis of uniform and tapered rotating beams using spectrally formulated finite elements, International Journal of Solids and Structures 44 (2007) 5875–5893.
[16] C.A. Dorao, H. Jakobsen, A parallel time-space least-squares spectral element solver for incompressible flow problems, Applied Mathematics and Computation 185 (2007) 45–58.
[17] G. Tohumoglu, Analysis of periodically time-varying discrete-time systems in spectral domain, Applied Mathematics and Computation 162 (2005) 1151–1165.
[18] D. Givoli, B. Neta, I. Patlashenko, Finite element analysis of time-dependent semi-infinite wave-guides with high-order boundary treatment, International Journal for Numerical Methods in Engineering 58 (13) (2003) 1955–1983, doi:10.1002/nme.842.
[19] L. Kucherov, D. Givoli, High-order absorbing boundary conditions incorporated in a spectral element formulation, International Journal for Numerical Methods in Biomedical Engineering. doi:10.1002/cnm.1188.
[20] J.M. Lindquist, B. Neta, F.X. Giraldo, A spectral element solution of the Klein–Gordon equation with high-order treatment of time and non-reflecting boundary, Wave Motion 47 (5) (2010) 289–298, doi:10.1016/j.wavemoti.2009.11.007.
[21] J.M. Lindquist, Unstructured high-order Galerkin-temporal-boundary method for the Klein–Gordon equation with non-reflecting boundary conditions, Ph.D. dissertation, Naval Postgraduate School, Monterey, California, 2010.
[22] V. van Joolen, D. Givoli, B. Neta, High-order non-reflecting boundary conditions for dispersive waves in cartesian, cylindrical and spherical coordinate systems, International Journal of Computational Fluid Dynamics 17 (4) (2003) 263–274.
[23] J. Pedlosky, Geophysical Fluid Dynamics, second ed., Springer, Verlag, New York, 1986.
[24] V.J. van Joolen, Application of higdon non-reflecting boundary conditions to shallow water models, Ph.D. dissertation, Naval Postgraduate School, Monterey, California, 2003.
[25] T. Hagstrom, S.I. Hariharan, A formulation of asymptotic and exact boundary conditions using local operators, Applied Numerical Mathematics 27 (4) (1998) 403–416. <http://dx.doi.org/10.1016/S0168-9274(98)00022-1>.
[26] L.L. Thompson, R. Huan, Accurate radiation boundary conditions for the two-dimensional wave equation on unbounded domains, Computer Methods in Applied Mechanics and Engineering 191 (1) (2001) 311–351.
[27] V.J. van Joolen, B. Neta, D. Givoli, High-order higdon-like boundary conditions for exterior transient wave problems, International Journal for Numerical Methods in Engineering 63 (7) (2005) 1041–1068, doi:10.1002/nme.1322.
[28] A.R. Curtis, High-order explicit Runge–Kutta formulae, their uses, and limitations, IMA Journal of Applied Mathematics 16 (1975) 35–53, doi:10.1093/imamat/16.1.35.